Chemical Physics Letters 488 (2010) 54–56

Contents lists available at ScienceDirect

Chemical Physics Letters

journal homepage: www.elsevier.com/locate/cplett

Photoluminescence of barium–calcium titanates obtained by the microwave-assisted hydrothermal method (MAH)

A.E. Souza [a,*], R.A. Silva [a], G.T.A. Santos [a], M.L. Moreira [b], D.P. Volanti [c], S.R. Teixeira [a], E. Longo [c]

[a] DFQB, UNESP, Univ. Estadual Paulista, 19060-080 Presidente Prudente, SP, Brazil
[b] LIEC, Depto. de Química, UFSCar, Univ. Federal de São Carlos, São Carlos, SP, Brazil
[c] LIEC, IQ, UNESP, Univ. Estadual Paulista, Araraquara, SP, Brazil

ARTICLE INFO

Article history:
Received 28 November 2009
In final form 26 January 2010
Available online 1 February 2010

ABSTRACT

$Ba_{1-x}Ca_xTiO_3$ (x = 0, 0.25, 0.50, 0.75, and 1.0) samples report the association of three types of clusters synthesized by the microwave-assisted hydrothermal at 140 °C for 40 min. In order to evaluate influence of structural order–disorder degree among them, photoluminescence (PL) emission, X-ray diffraction, FT-Raman spectroscopy and Ultraviolet–Visible absorption were used. The PL emission of the crystalline phases grows up with the calcium concentration and reaches the highest PL emission to 0.75 Ca concentration, which is supported by the symmetry break caused by the phase transition. This PL emission is higher than that of the $CaTiO_3$ phase.

1. Introduction

Potential applications enhance the importance of $ATiO_3$ (A = Ca, Ba, Sr, and Pb) compound as ferroelectric, semiconductor and catalytic materials [1–3]. Although, the ceramic properties of the barium titanate ($BaTiO_3$) have been widely investigated, more recently there is an interest in studying nanoscale particles with tetragonal structure, due to the properties which depend strongly on the crystalline structure and grain size.

$BaTiO_3$ (BT) nanoparticles can be prepared by several methods [4–8]; among the chemical methods, the hydrothermal is one of the promising routes for production of oxides with extremely fine particles, with different morphology and homogeneous distribution of grain sizes [3,8–13]. In recent publication [14] it was observed that $CaTiO_3$ powders synthesized using the MAH method show that intermediate energy states within the band gap are mainly responsible for photoluminescence (PL) emission. Also, $SrZrO_3$ and $SrTiO_3$ [15,16] powders and multilayer thin films, prepared using other methods, present PL emission at different colors which can be associated to numerous states within the forbidden band gap.

Besides the several works about binary titanates, no one research has been reported on the preparation of ternary titanates using MAH method. In this work, the microwave radiation associated with hydrothermal method was employed to obtain ternary $Ba_{1-x}Ca_xTiO_3$ (x = 0, 0.25, 0.50, 0.75, and 1.0) compounds under friendly conditions, producing ordered and disordered PL materials with visible broad-band centered at green region.

2. Experimental

Barium–calcium titanates (BCT) were prepared according to procedure: $(0.01 - x)$ mol $BaCl_2{\cdot}2H_2O$ and (x) mol $CaCl_2{\cdot}2H_2O$ (x = 0, 0.0025, 0.0050, 0.0075, and 0.01) were dissolved in 20 mL of deionized water within the Teflon® cup of the MAH reaction chamber. With constant stirring and under nitrogen gas bubbling, 0.01 mol of $C_{12}H_{28}TiO_4$ was added to the solution, and after stirring for 10 min at room temperature, 50 ml of KOH (6 mol) was quickly added to act as a mineralization agent. Afterward the cup was put within the reaction chamber which was sealed and installed inside the microwave oven. The synthesis process was carried out at 140 °C for 40 min (at a heating rate of 140 °C/min) and maximum pressure of 4 bar. The system was cooled to room temperature and the powder ceramic was washed in deionized water and centrifuged several times until neutral pH (pH 7). The crystalline powder was dried at 110 °C for 12 h. The as-synthesized powders were characterized by X-ray diffraction (Rigaku, model D/Max-2500/PC), Cu Kα radiation, with a scan speed of 4°/min and a step width of 0.02°. Raman spectra were obtained using a micro-Raman Renishaw spectrograph model inVia equipped with a Leica microscope (50× objectives with ~1 μm² spatial resolution) and CCD detector. Scan ranges of 100–1400 cm^{-1}, using the 633 nm wavelength of a He–Ne laser. Photoluminescence (PL) spectra were collected with a Thermal Jarrel-Ash Monospec 27 monochromator and a Hamamatsu R446 photomultiplier. The 350.7 nm exciting wavelength of a krypton ion laser (Coherent Innova) was used; the nominal output power of the laser was kept at 200 mW.

* Corresponding author. Address: Rua Roberto Simonsen 305, 19060-080 Presidente Prudente, SP, Brazil. Fax: +55 18 3221 5682.
E-mail addresses: agda@fct.unesp.br, agda_pb@ig.com.br (A.E. Souza).

0009-2614/$ - see front matter © 2010 Elsevier B.V. All rights reserved.
doi:10.1016/j.cplett.2010.01.065

Ultraviolet–Visible (UV–Vis) spectroscopy for the spectral dependence of optical absorbance of all samples was taken using a Cary 5G UV–Vis NIR Spectrophotomer in the total reflection mode. Two reference standards Labsphere Certified Reflectance (SRS 94-010 and SRD 02-010) were used. All measurements were taken at room temperature.

3. Results and discussion

X-ray diffraction patterns (Fig. 1) show tetragonal perovskite structure (PDF 83-1878) and a small amount of barium carbonates (PDF 01-0506) for the composition $Ba_{1-x}Ca_xTiO_3$ with $x < 1$. The tetragonal phase can be denoted by the peak nearby $2\theta = 45°$. In this case, the splitting of the cubic (2 0 0) into tetragonal (2 0 0) and (0 0 2) reflections was observed, indicating the high tetragonality of this sample. In addition, for concentrations $x = 0.50$ and 0.25, orthorhombic barium/calcium carbonate $BaCa(CO_3)_2$ (PDF 03-0322) was identified in these samples. XRD data show the presence of a pure $CaTiO_3$ (CT) orthorhombic perovskite phase (PDF 82-0229), to $x = 1$ (CT) which was also observed by Marques et al. [17] using polymeric precursor method and Moreira et al. using the MAH method [3]. For $x = 0.75$ concentration, the diffraction peaks show only the calcium carbonate formation $CaCO_3$ (PDF 01-0837) and, the halo near $2\theta = 30°$ in the X-ray pattern indicates the formation of titanate with short-range order. This result was confirmed in two new samples which were prepared, one at the same previous conditions and other with a shorter treatment time (10 min). The results show that $x = 0.75$ is the worse concentration for the obtaining of pure BCT phase.

Fig. 2 shows Raman spectra of the BCT to different compositions. The peak at 305 cm^{-1} in the samples with Ba indicates the tetragonal BT phase formation is the dominate phase [3]. The mode at 716 cm^{-1} is related to the highest frequency longitudinal optical mode. The higher relative intensity of the band in comparison with the other tetragonal bands for nanoparticles can be related to Ba^{2+} defects in the BT lattice [3]. The peaks at 515, 262, and 180 cm^{-1} are assigned to the fundamental TO mode of A_1 symmetry which comprise the main difference in Raman spectra among tetragonal and orthorhombic phase of BT. The asymmetry in the peak at 515 cm^{-1} suggests the existence of coupling of TO modes associated with the tetragonal phase. The presence of these peaks in the Raman spectrum indicates a tetragonal structure to the BT and is in agreement with XRD data [3]. The short peak at 1060 cm^{-1} confirms the presence of a small amount $BaCO_3$ in all samples. This peak disappears when the calcium concentration is raised as confirmed by XRD and Raman data. The Raman modes

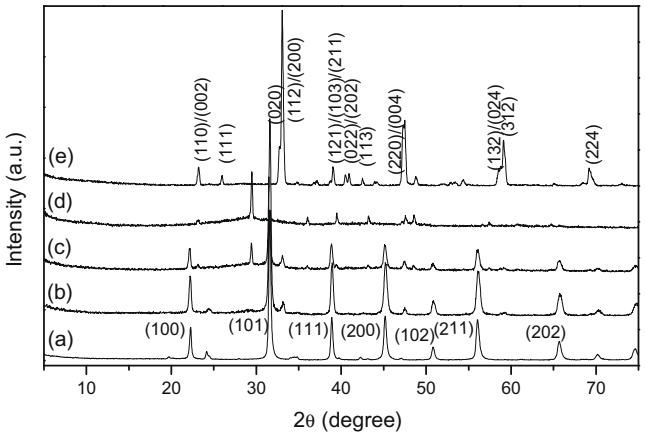

Fig. 1. XRD patterns of the $Ba_{1-x}Ca_xTiO_3$ sample: (a) $x = 0$; (b) $x = 0.25$; (c) $x = 0.50$; (d) $x = 0.75$; (e) $x = 1$.

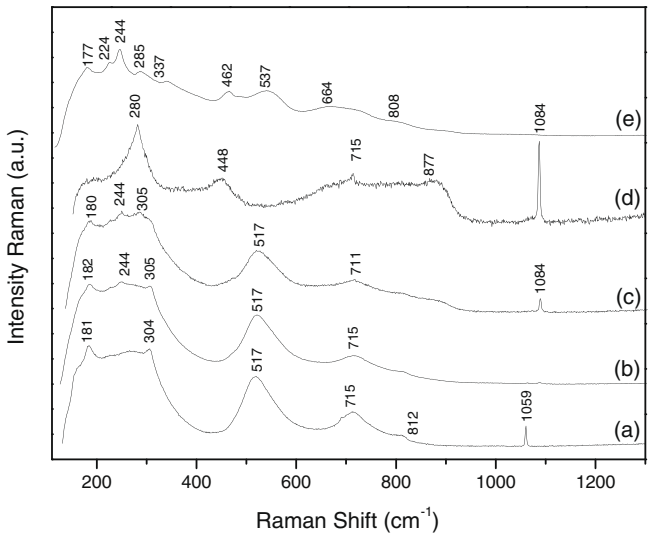

Fig. 2. Raman spectra of the $Ba_{1-x}Ca_xTiO_3$ sample: (a) $x = 0$; (b) $x = 0.25$; (c) $x = 0.50$; (d) $x = 0.75$; (e) $x = 1$.

from $x = 0$ to 0.50 are characteristic of the barium titanate. Sample with $x = 0.75$ shows a Raman spectra different of the other samples, characterizing the new phase not identified by XRD data.

The nine CT Raman modes observed in the range from 145 to 815 cm^{-1} are attributed orthorhombic structures which are in agreement with the literature [18]. The Raman mode from 177 to 337 cm^{-1}, is attributed to the O–Ti–O bending modes. The 462 and 537 cm^{-1} are ascribed to the torsional mode, and 664 cm^{-1} is assigned to the Ti–O symmetric stretching vibration. As shown by Cavalcante et al. [18], the positions of the peaks in Raman spectrum have a small shift according to the method used to prepare the compounds. Also, the stoichiometric composition can change the peak positions and the intensities.

According to Fig. 1, the XRD patterns of the three intermediary compositions ($x = 0.25$, 0.50, and 0.75) show a band around $2\theta = 30°$ indicating that these samples still present a small structural disorder. The XRD pattern of the $Ba_{0.25}Ca_{0.75}TiO_3$ sample shows only the $Ca(CO)_3$ crystalline phase and the band which characterizes a short-range order structure. XRD data serve to explain PL results. The PL property is affected by the relationship between short and long-range structural lattice order–disorder [19]. Considering that calcium carbonate does not have a significant influence on the PL emission, the very high PL intensity of this sample (Fig. 3) can be associated with the existence of two cubic–octahedral clusters. These clusters have a quite different charge distribution for BaO_{12} and CaO_{12}, which are presents in singular ratios for each sample, and they are associated under different conditions with an octahedral TiO_6 cluster. Also, it is observed that the PL spectrum maximum shifts to a higher λ (nm), and its intensity increases with the calcium concentration, indicating that the CaO_{12} cluster introduces a break of local symmetry in the tetragonal lattice and produces new orthorhombic structures. As the PL provides information about ions in relation to their neighborhood (i.e., about their clusters associations), the higher PL intensity in the $Ba_{0.25}Ca_{0.75}TiO_3$ composition must be related to the disorder introduced by structural changes and the amount of the disordered phase (short and medium-range disorder) present in this material. All the samples present the maximum component emission around the green light range (between 495 and 545 nm).

Three types of additional energy levels exist in the forbidden band of titanates: free-exciton levels, STE levels and defect or impurity levels; all energy levels are near to the conduction band

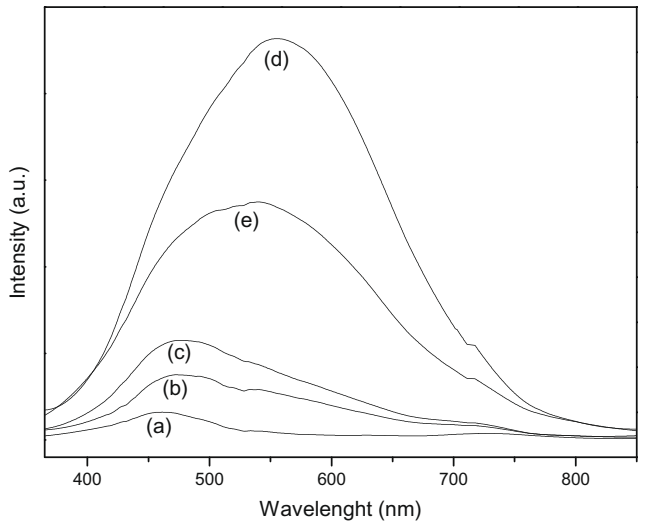

Fig. 3. Photoluminescence spectra of the $Ba_{1-x}Ca_xTiO_3$ sample: (a) $x = 0$; (b) $x = 0.25$; (c) $x = 0.50$; (d) $x = 0.75$; (e) $x = 1$.

Table 1
Average grain size of the $Ba_{1-x}Ca_xTiO_3$ samples.

Samples	Band gap (eV)	Crystallite size (nm) [20]
$BaTiO_3$	3.36	39
$Ba_{0.75}Ca_{0.25}TiO_3$	3.24	34
$Ba_{0.50}Ca_{0.50}TiO_3$	3.44	17
$Ba_{0.25}Ca_{0.75}TiO_3$	3.78	N.I.*
$CaTiO_3$	3.51	45

* N.I.: phase not identified by XRD.

[20]. The values of the gap energies can be obtained by the Wood and Tauc method [21]. The band gap determined from UV–Vis absorption for all samples is between 3.24 and 3.78 eV (Table 1). The PL excitation energy used in the present work (3.52 eV corresponding to 350 nm) is of the same order as these band gaps, so it is difficult for an electron in the valence band to be directly excited to the conduction band, mainly due to thermal effects. Therefore, it is likely that the electrons were excited first to the localized levels within the forbidden gap and, then the observed broadbands in PL emissions do not result from the free-exciton recombination. In this work, we observed poly- and nanocrystalline oxide where oxygen vacancies are known to be the most common defects which usually act as radiative centers in luminescence processes [22–24].

The broad luminescent band usually observed at low temperatures in perovskite-type crystals is associated with the presence of imperfections or defects and is typical of multiphonon and multilevel process. The literature includes several papers explaining favorable conditions for PL emission in materials presenting a degree of order–disorder. The authors attributed the radiative decay process to distorted octahedral, self-trapped excitons, oxygen vacancies, surfaces states and a charge transfer via intrinsic defects inside an oxygen octahedron [20].

Table 1 shows band gap energies obtained from UV–Vis spectra of the BCT with different compositions. These values show that for $x = 0.25$, the band gap to BCT phase is smaller than to BT ($x = 0$) phase, suggesting that the BCT phase has a higher degree of order–disorder than the BT phase. This occurs because the BT tetragonal structure is disordered by the CaO_{12} clusters making available additional electronic levels in the forbidden band gap. For $x = 0.50$, the high structural distortion can result in a higher band gap value than in the prior phases. For $x = 0.75$, the band gap has the highest calculated value which could be associated with the structural threshold among tetragonal and orthorhombic phases. For the intermediate phases (0.25–0.75), it is observed that the band gap energy rises with the Ca concentration.

4. Conclusions

The results reported here illustrate the use of the MAH method in the synthesis of barium–calcium titanates. They show that the tetragonal BCT phase can be obtained under calcium concentrations of 0.25 and 0.50. For 0.75, there is no formation of titanate with long-range order due to be the threshold of tetragonal–orthorhombic phase transition. The samples present PL emission in the visible green region. The PL emission of the BCT phase rises with the calcium concentration and has the highest value for 0.75 which is higher than the calcium titanate value. The higher PL emission is supported by the symmetry break caused by the phase transition that occurs with this concentration of calcium.

Acknowledgements

The authors gratefully acknowledge Danilo Cardoso Ferreira and José Leopoldo Costantino for Raman data and FAPESP, CAPES and, CNPq for financial support.

References

[1] F.V. Motta, A.P.A. Marques, J.W.M. Espinosa, O.S. Pizani, E. Longo, J.A. Varela, Curr. Appl. Phys. 10 (2010) 16.
[2] N. Baskaran, H. Chang, Mater. Chem. Phys. 77 (2002) 889.
[3] M.L. Moreira et al., Chem. Mater. 20 (2008) 5381.
[4] E. Orhan et al., Phys. Rev. 71 (2005) 0851131.
[5] Z. Xinhua, W. Junyi, Z. Zhenghai, Z. Jianmin, Z. Shunhua, L. Zhiguo, M. Naiben, J. Am. Ceram. Soc. 91 (2008) 1.
[6] W.S. Cho, J. Phys. Chem. Solids 59 (1998) 659.
[7] P. Durán, D. Gutierrez, J. Tartaj, M. Bañares, C. Moure, J. Eur. Ceram. Soc. 22 (2002) 797.
[8] K. Sridhar, Curr. Sci. 85 (2003) 1730.
[9] F.I. Pires, E. Joanni, R. Savu, M.A. Zaghete, E. Longo, J.A. Varela, Mater. Lett. 62 (2008) 239.
[10] Z. Chen, W. Li, W. Zeng, M. Li, J. Xiang, Z. Zhou, J. Huang, Mater. Lett. 62 (2008) 4343.
[11] M.L. Santos, R.C. Lima, C.S. Riccardi, R.L. Tranquilin, P.R. Bueno, J.A. Varela, E. Longo, Mater. Lett. 62 (2008) 4509.
[12] D.P. Volanti et al., J. Alloys Compd. 459 (2008) 537.
[13] L.S. Cavalcante, J.C. Sczancoski, J.W.M. Espinosa, J.A. Varela, O.S. Pizani, E. Longo, J. Alloys Compd. 474 (2009) 195.
[14] M.L. Moreira et al., Acta Mater. 57 (2009) 5174.
[15] V.M. Longo et al., Theor. Chem. Acc. 124 (2009) 385.
[16] M.L. Moreira, J. Andrés, V.M. Longo, M.S. Li, J.A. Varela, E. Longo, Chem. Phys. Lett. 473 (2009) 293.
[17] V. Marques et al., Solid State Sci. 10 (2008) 1056.
[18] L.S. Cavalcante et al., Chem. Eng. J. 143 (2008) 299.
[19] F.V. Motta et al., J. Lumin. 129 (2009) 686.
[20] W.F. Zhang, Z. Yin, M.S. Zhang, Z.L. Du, W.C. Chen, J. Phys. Condens. Mater. 11 (1999) 5655.
[21] D.L. Wood, J. Tauc. Phys. Rev. 5 (1972) 3144.
[22] K. Vanheusden, W.L. Warren, J.A. Voigt, C.H. Seager, D.R. Tallant, Appl. Phys. Lett. 67 (1995) 1280.
[23] L. Foress, M. Schubnell, Appl. Phys. B 56 (1993) 363.
[24] Y.C. Zhu, C.X. Ding, G.H. Ma, Z.L. Du, J. Solid State Chem. 139 (1998) 124.